

Haverford College

Haverford Scholarship

Faculty Publications

Chemistry

2008

Sustainable energy from deep ocean cold seeps

Mark E. Nielsen

Clare E. Reimers

Helen K. White

Haverford College, hwhite@haverford.edu

Sonam Sharma

Follow this and additional works at: https://scholarship.haverford.edu/chemistry_facpubs

Repository Citation

Nielsen, M.E., C.E. Reimers, H.K. White, S. Sharma and P.R. Girguis. (2008) Sustainable energy from deep ocean cold seeps . *Energy & Environmental Science* 1 : 584 - 593.

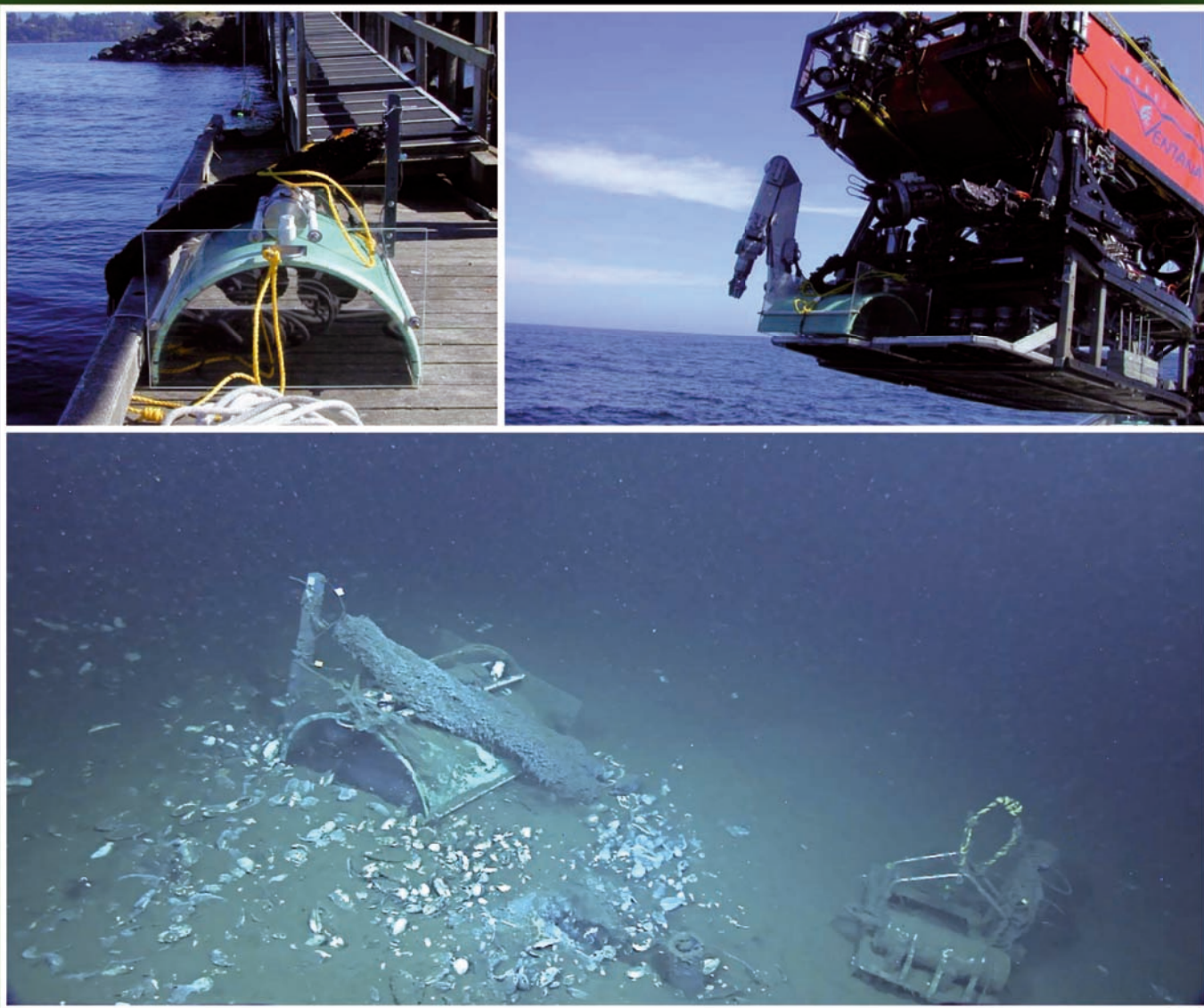
This Journal Article is brought to you for free and open access by the Chemistry at Haverford Scholarship. It has been accepted for inclusion in Faculty Publications by an authorized administrator of Haverford Scholarship. For more information, please contact nmedeiro@haverford.edu.

Energy & Environmental Science

www.rsc.org/ees

Volume 1 | Number 5 | November 2008 | Pages 513–596

Downloaded on 22 March 2013
Published on 15 September 2008 on http://pubs.rsc.org | doi:10.1039/B811899J



ISSN 1754-5692

RSC Publishing

COVER ARTICLE

Mark Nielsen *et al.*
Sustainable energy from deep ocean cold seeps

MINIREVIEW

Janusz Nowotny
Titanium dioxide-based semiconductors for solar-driven environmentally friendly applications: impact of point defects on performance

Sustainable energy from deep ocean cold seeps

Mark E. Nielsen,^{*a} Clare E. Reimers,^{*a} Helen K. White,^b Sonam Sharma^b and Peter R. Girguis^b

Received 11th July 2008, Accepted 28th August 2008

First published as an Advance Article on the web 15th September 2008

DOI: 10.1039/b811899j

Two designs of benthic microbial fuel cell (BMFC) were deployed at cold seeps in Monterey Canyon, CA, unattended for between 68 and 162 days. One design had a cylindrical solid graphite anode buried vertically in sediment, and the other had a carbon fiber brush anode semi-enclosed in a chamber above the sediment–water interface. Each chamber included two check valves to allow fluid flow from the sediment into the chamber. On average, power outputs were 0.2 mW (32 mW m⁻² normalized to cross sectional area) from the solid anode BMFC and from 11 to 56 mW (27–140 mW m⁻²) during three deployments of the chambered design. The range in power produced with the chambered BMFC was due to different valve styles, which appear to have permitted different rates of chemical seepage from the sediments into the anode chamber. Valves with the lowest breaking pressure led to the highest power production and presumably the highest inputs of electron donors. The increase in power coincided with a significant change in the microbial community associated with the anode from being dominated by epsilonproteobacteria to a more diverse community with representatives from deltaproteobacteria, epsilonproteobacteria, firmicutes, and flavobacterium/cytophaga/bacterioides (FCB). The highest levels of power delivered by the chambered BMFC would meet the energy requirements of many oceanographic sensors marketed today. In addition, these BMFCs did not exhibit signs of electrochemical passivation or progressive substrate depletion as is often observed with buried anodes.

Introduction

Natural redox gradients between anoxic sediments and overlying water have recently been used to produce electrical power *in situ* through benthic microbial fuel cells (BMFCs).^{1–9} BMFCs couple the oxidation of reduced compounds in sediments to the reduction of oxygen dissolved in the overlying water. Microorganisms play several roles in these systems including: maintenance of the redox gradient, production of redox mediators, generation of electron-rich metabolites (*e.g.* sulfide ions), and in some cases, delivery of electrons to an electrode through direct electron transfer.^{10–16}

Many ocean sensors have low power requirements, which make them appropriate applications for microbial fuel cell

technology.^{1,4,17–19} However, challenges in developing BMFCs for functional underwater applications have included: (1) relatively modest supply rates of natural fuels from the environment, (2) passivation of electrode surfaces by the adsorption of reaction products,²⁰ and (3) the energy cost of enhancing fuel availability (by pumping for example).⁷ Also, most microbial fuel cell experiments are performed on a small scale and do not produce useful amounts of power (*i.e.* when not normalized to electrode surface area, chamber volume or device cross sectional area). The most common method for addressing these challenges is refinement of the fuel cell itself, involving testing of different device configurations, electrode materials and/or schemes for delivering more fuel to the anode. Another method is to target environments where natural phenomena can help drive the transport of reduced compounds to the anode of the BMFC.

In this paper we describe an experimental program of BMFC testing at seafloor locations with chemical seepage. Results from two tests described in this paper were presented previously in a different form as ancillary data.⁷ Here they are discussed

^aCollege of Oceanic and Atmospheric Sciences, Hatfield Marine Science Center, Oregon State University, Newport, OR, 97365, USA. E-mail: mnielsen@coas.oregonstate.edu; creimers@coas.oregonstate.edu

^bHarvard University, Biological Labs, 16 Divinity Avenue, Cambridge, MA 02138, USA

Broader context

Long-term monitoring is an important aspect of modern oceanography. One challenge of such monitoring is that many sensors have a service life limited by the batteries that power them. Benthic microbial fuel cells (BMFCs) have been proposed as persistent power supplies that could power sensors in remote off-grid environments. BMFCs generate power from the natural redox gradient that occurs across the sediment–water interface. This paper describes a field program of BMFC deployments that included different electrode materials and fuel cell configurations. One of the designs produced power at a level relevant for powering sensors. The processes that deliver electron donors to the BMFCs are discussed in detail, and we include analyses of the microbial communities associated with the BMFCs.

in-depth with additional measurements and attention paid to environmental processes that control the supply of electron donors to the anode (diffusion and/or advection). Without the input of energy to pump fluid (or otherwise manipulate parts of the fuel cell) one BMFC produced usable amounts of power, relying on natural processes in marine sediments to provide electron donors to the anode. The microbial phylogeny of biofilms sampled from anode materials was investigated, and the highest diversity was observed in the BMFC with the highest power production.

Power targets for BMFCs

Long-term monitoring is important to many environmental and oceanographic investigations. To meet this objective, sensors and supporting communication devices are evolving to use less and less power, thus extending available deployment times in remote, “off grid”, locations. Table 1 presents examples of sensors and a telesear modem with low power requirements that are relevant to oceanographic studies. Power requirements for such devices are typically not static and depend on the duty cycle and the extent of data processing, storage and/or communication. Currently, batteries are the power supply of choice in deep ocean settings where other alternatives such as wind or solar are not available. Batteries have a finite life, however, so a development goal for benthic microbial fuel cells is to replace batteries in selected long-term monitoring applications. The sensors listed in Table 1 typically consume from 20 mW to a little less than 500 mW during periods of peak demand. The BMFCs described in this paper should be evaluated in the context of the power range.

Regional setting

The locations for these experiments were within the Monterey Submarine Canyon, CA (Fig. 1). This canyon is a prominent

Table 1 Examples of power requirements for oceanographic sensors and communication devices

Instrument	Manufacturer	Voltage/V	Power requirement/mW
Turbidity meter	Seapoint Sensors, Inc.	7–20	24.5 avg, 42 peak
Chlorophyll-a fluorometer	Seapoint Sensors, Inc.	8–20	120 avg, 216 peak
Conductivity, temperature and depth	Ocean Sensors, Inc.	6	1.2 sleep mode, 420 peak
Backscattering meter	Wetlabs, Inc.	7–15	0.6 sleep mode, 560 peak
Wireless temperature probe/transmitter	Madgetech, Inc.	3.3	49.5
Acoustic receiver	Sonotronics, Inc.	3.5	14 standby, 28 peak
Acoustic modem	Teledyne Benthos	14–28	12 standby, 500 active, 20 W transmit

geomorphic feature on the west coast of North America. The canyon system begins near shore and extends to a water depth of approximately 3.5 km. Cold seeps characterized by vesicomid clams and chemoautotrophic bacterial mats are ubiquitous in the canyon.^{21–23} It has been suggested that the seepage is driven by tectonic compression from transform faults between the Pacific and North American plates or by “slow mud-diapirism”.²⁰ The canyon cuts into the organic-rich Monterey Formation, which is thought to be the source of organic carbon in the seep fluid.²⁴ The study area for these experiments is known as Extrovert Cliff (36° 46.6'N, 122° 05.1'W) and is characterized by a muddy slope with cold seeps that affect patches of seafloor (~1–10 m²) spaced 10's of meters apart, at a depth of about 960 m (Fig. 2). Flow intensity from the seeps varies spatially and temporally with some seeps exhibiting little detectable advection and others having a discrete conduit where active flow results in a shimmering fluid expulsion across the sediment–water interface. Sensors mounted on a remotely operated vehicle (ROV) used during these experiments indicated a bottom water temperature of 4 °C, a salinity of 34.5 and dissolved oxygen concentration of approximately 11 μM directly over the seeps.

Seeps as energy sources

Reduced compounds in pore fluids from cold seeps can be converted to electrical power by a BMFC by both biological and chemical mechanisms of electron transfer.²⁰ The amount of electrical power produced depends on fluid composition, transport of electrochemical reactants and products to and from the electrodes, and the design of the BMFC including size and electrode surface area. Furthermore, these factors can depend on each other; for example, the dominant transport process may be affected by the design of the BMFC. In previous experiments at these seeps, we used a solid graphite anode buried in the sediment.²⁰ The power record from that experiment was characterized by a peak (about 25 days into the deployment) and then decay to a low quasi-steady state level of power production. Decaying production of power over time is consistent with diffusion as the dominant mode of transport of electron donors to the anode, resulting in depletion of electron donors at the electrode surface and/or passivation of the electrode. It also implies that advective transport through fluid seepage was insufficient to prevent these effects. Entering into this study we hypothesized that: (1) burying an anode may restrict or redirect localized advection through the sediment; and (2) a BMFC design which allowed natural seepage to influence the anode environment should produce significantly more power.

Labonte *et al.* recently deployed benthic flux chambers in Monterey Canyon over seeps very close to the areas that we targeted in this experimental program.²⁵ The chambers that covered 640 cm² of seafloor did not impede flow and measured fluid flow rates of 2–6 × 10³ cm y⁻¹ for the most vigorous seeps (corresponding to volumetric fluxes of 2.4–7.3 cm³ s⁻¹ seep⁻¹). The concentration of sulfide in the seep fluids is approximately 12 mM.²⁰ Thus if we assume that sulfide is the primary electron donor, the maximum current (*I*, A) that might be generated by a BMFC designed similar to a flux chamber placed over an active seep may be estimated as:

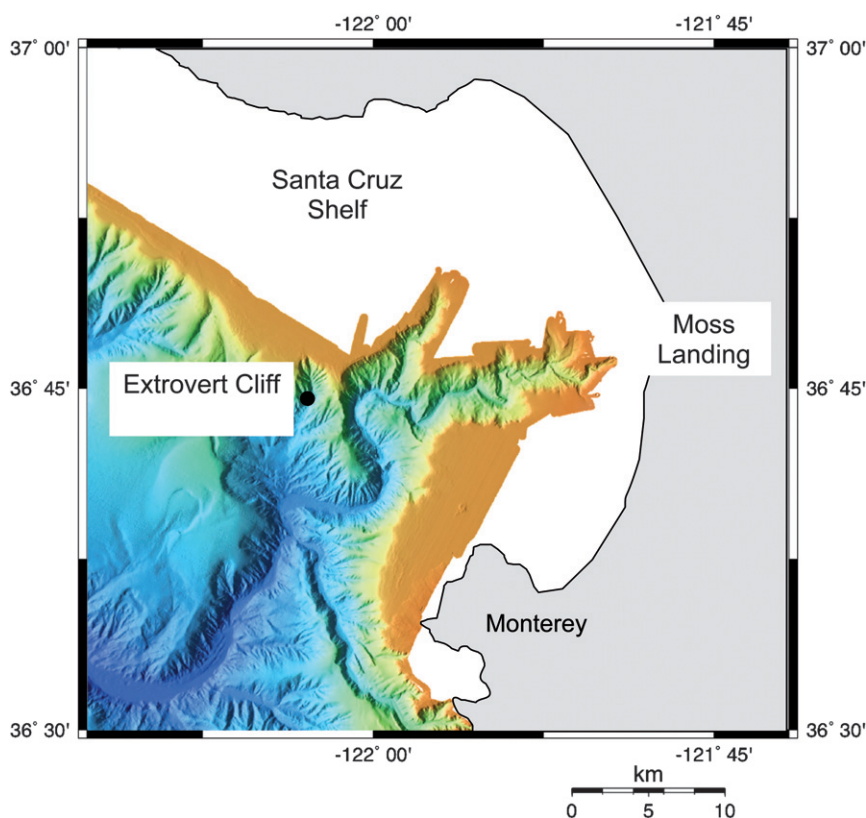


Fig. 1 Location of study site within Monterey Canyon. Adapted from bathymetry survey by Monterey Bay Aquarium Research Institute (<http://www.mbari.org/data/mapping/monterey/default.htm>).

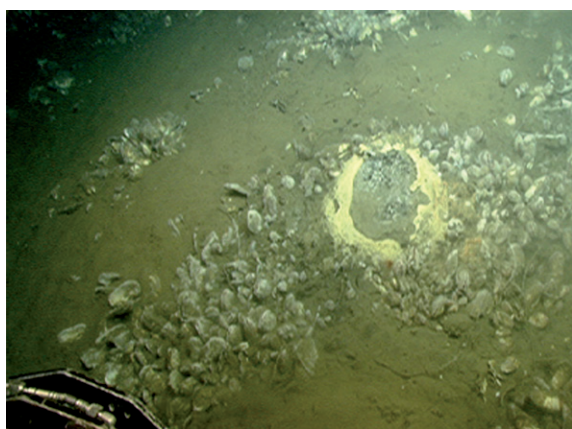


Fig. 2 Image of seeps at Extrovert Cliff in Monterey Canyon. Clams indicate seepage areas along a sloped seabed. A conduit for vigorous fluid flow is visible in the right portion of the photo ringed with a bacterial mat.

$$I = Q \times C_0 \times n \times F \quad (1)$$

where Q is the volumetric fluid flux ($\text{cm}^3 \text{s}^{-1}$), C_0 is the concentration of electron donor in the fluid (mol cm^{-3}), n is the number of electrons involved in electrochemical reaction (2, in the case of sulfide oxidation to sulfur) and F is Faraday's constant ($96\,485 \text{ C mol}^{-1}$). Assuming 100% current efficiency and a BMFC voltage fixed at 0.4 V, the maximum power sustainable by Monterey Canyon seeps can be calculated as the product of current and

voltage. These calculations predict power outputs of 37 to 112 mW.

In contrast, in the absence of seepage the current would tend to be limited by diffusion across the sediment–water interface and proportional to the seafloor area (A) enclosed by a chambered BMFC. In this case, the current can be approximated using:

$$I = n \times F \times \phi D_s \frac{d\bar{C}}{dz} \times A \quad (2)$$

where ϕ represents the sediment porosity ($\text{cm}^3_{\text{porewater}} \text{cm}^{-3}_{\text{sediment}}$), $d\bar{C}/dz$ denotes a spatially averaged concentration gradient of the dominant electron donor C across the sediment–water interface ($\text{mol cm}^{-3} \text{cm}^{-1}$), and D_s is the diffusion coefficient ($\text{cm}^2 \text{s}^{-1}$) for C corrected for sediment tortuosity effects.^{26,27} Beneath a chambered BMFC, concentration gradients may grow or shrink depending the rate of electron donor oxidation at the anode, the volume of the subsurface fluid reservoir supplying the sediment gradient, and perturbations caused by bioirrigation. We estimate that a diffusive flux across the sediment–water interface according to eqn (2) would result in power output ranging from 1 to 26 mW (again assuming a current efficiency of 100% and an operating voltage of 0.4 V). The large range is due to expected variability in ϕ (0.6–0.9)²⁸ which leads to a range in D_s from 5.6 to 9.3×10^{-6} (calculated according to Schulz²⁷) and variability in $d\bar{C}/dz$. We estimated $d\bar{C}/dz$ would range from 1 to $10 \times 10^{-6} \text{ mol cm}^{-3} \text{cm}^{-1}$ based on sulfide profiles measured in sediment cores of seep sediments by Rathburn *et al.*²⁹

Methods and instrumentation

Benthic microbial fuel cells

The BMFCs in this study were deployed with the *ROV Ventana* operated by the Monterey Bay Aquarium Research Institute. Vigorous seeps with visible fluid flow were targeted for all deployments. The fuel cells differed primarily in their anodes: BMFC 1 had a single solid graphite anode buried in the mud, and BMFCs 2–4 had carbon-fiber brush anodes suspended above the sediment–water interface inside a benthic chamber. BMFC 4 was a re-deployment of BMFC 2 with a slightly different configuration (details below).

The anode of BMFC 1 was constructed from a cylindrical piece of solid graphite (50 cm long with one end milled into a tip) and a diameter of 0.04 m (geometric surface area = 0.05 m²). A titanium bolt wrapped with the exposed end of an insulated copper wire was threaded into the upper end of the graphite and potted in a PVC sleeve with marine grade epoxy in order to make a connection to the circuit. The cross sectional area of the anode assembly (including the PVC sleeve) was 6.2×10^{-3} m². The cathode was a 0.5 m length of carbon-fiber brush electrode³⁰ fastened to a post that extended approximately 0.3 m above the sediment–water interface. A bare-wire Ag/AgCl reference electrode was also fastened to the cathode post. A pressure housing containing the control and measurement circuitry (described below) was attached with the cathode to a stainless steel frame placed on the seafloor. The anode was pushed vertically into the sediment into an active seepage conduit with a manipulator arm of the ROV.

The chambers (Fig. 3) were constructed from a section of acrylonitrile butadiene styrene (ABS) plastic sewer pipe (0.61 m id) cut lengthwise giving a rectangular cross sectional area of 0.4 m² (and an estimated chamber volume above the sediment of 2.0×10^{-2} m³ after it was pushed into the sediment). The ends of the chambers were made from 1.25 cm-thick acrylic, glued to the pipe section, and reinforced with stainless steel screws. Two one-way valves were installed on the top of each chamber to allow flow from the sediment into and through the chamber. Each chamber had a single anode consisting of three 1 m sections of carbon-fiber brush electrode³⁰ (connected end to end). The anode sections were spaced side-by-side evenly inside the chamber and

attached to the chamber walls with polypropylene hardware. The cathode for each BMFC was made from four 1 m sections of identical carbon-fiber brush electrodes connected to each other by attaching one end to a common titanium bolt with an insulated copper wire from the BMFC circuit. The bolt was potted in epoxy to protect the copper wire from corrosion. The other ends of the cathodes were connected to another titanium bolt at a common point. The cathodes were fastened to posts that extended approximately 0.5 m above the sediment–water interface from one corner of each chamber. The manufacturer-reported surface area of the brush electrodes is 26 m² per meter of length, giving total surface areas of approximately 78 and 104 m², for the anode and cathode, respectively. Bare-wire Ag/AgCl reference electrodes (for monitoring anode and cathode potentials) were attached to the posts supporting the cathode just below the electrodes (approximately 40 cm above the sediment–water interface). The potential of the bare-wire Ag/AgCl reference electrode in seawater under the conditions at this site is estimated to be approximately 236 mV vs. the standard hydrogen electrode.²⁰ Titanium pressure housings contained the measurement and control circuitry (described below) and were attached to the top of each chamber.

Fig. 4 depicts the pressure housing, electrical controls and data loggers for these BMFCs. Whole-cell potential (cathode vs. anode), anode potential (anode vs. Ag/AgCl) and current (after conversion to a voltage) were measured every 10 min with voltage recorders (Madgetech, Warner, NH). Whole-cell potential was controlled with a potentiostat (NW Metasystems, Bainbridge Island, WA) to allow enough current to flow to maintain the whole cell potential at some predetermined setpoint (0.4 V for these experiments). If/when the whole-cell potential falls below the setpoint, the potentiostat opens the circuit allowing the natural redox gradient to recover until the setpoint is met again. In effect, the potentiostat acts as a variable external load that is automatically manipulated to maintain the predetermined voltage. Cathode potential was calculated from the whole-cell and anode potentials.

When BMFC 2 was recovered, we attached a syntactic foam float to the cathode assembly and replaced the spring loaded check valves with swing check valves that have a lower cracking pressure (0.7 kPa compared to 3.4 kPa) and re-deployed the

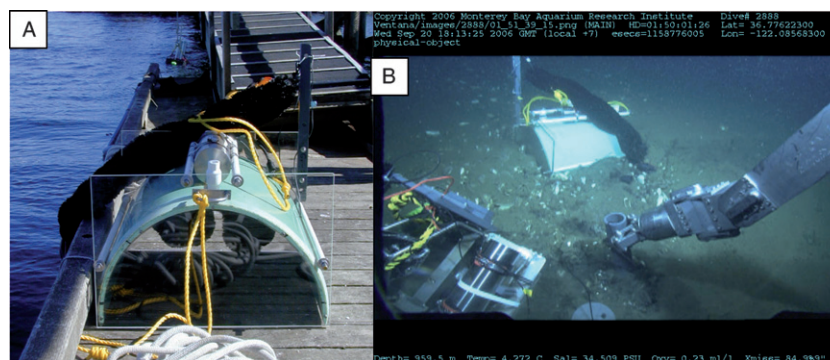


Fig. 3 Photographs of the chambered BMFC: (A) On the dock prior to a test deployment. The anodes can be seen suspended inside the chamber. The one-way valves, and the pressure housing that contains the controlling potentiostat and voltage loggers can be seen on top of the chamber. (B) Just after deployment on the seafloor in Monterey Canyon (photograph is a screen grab from the *ROV Ventana* high definition video system). In the foreground, the PVC sleeve supporting the solid anode from BMFC 1 is being pushed into the sediment.

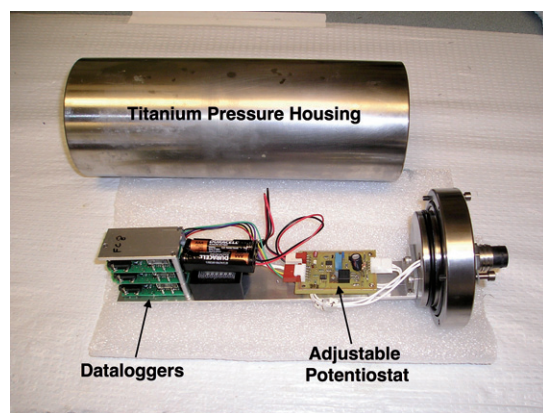


Fig. 4 Photograph of potentiostat that controls the whole-cell potential and the titanium pressure housing.

BMFC on the same footprint (± 0.1 m). This deployment is denoted BMFC 4.

Prior to the field deployments in Monterey Canyon, the chambered BMFCs (configured as BMFC 2 and 3) were tested in Yaquina Bay, OR. The tests in the bay served not only to verify proper operation of the BMFCs but also to condition the electrodes. The solid-anode BMFC was not tested and therefore the electrodes were not conditioned. BMFCs 1–3 were deployed in Monterey Canyon on a single cruise in September 2006. BMFC 1 was deployed for 162 days, and BMFCs 2 and 3 were deployed for 68 and 69 days, respectively. BMFC 2 was subsequently redeployed as BMFC 4 for an additional 127 days.

Microbiological community analysis

Clippings from the carbon fiber brush anodes from BMFC 2 and BMFC 4 were collected at the conclusion of the respective deployments. The samples were collected with flame-sterilized forceps and shears immediately upon recovery of the BMFCs to the deck of the ship. Approximately 2 g of fibers were clipped and preserved in a filter-sterilized 1 : 1 solution of ethanol and iso-osmotic, phosphate buffered saline and frozen at -50 °C. The anode of BMFC 1 could not be sampled because it broke off from its PVC sleeve and was lost during recovery.

Nucleic acids were extracted with the PowerSoil DNA extraction kit (MoBio Inc., San Diego, CA), modified to maximize yields.³¹ Small-subunit (SSU) rRNA bacterial genes from all samples were amplified by PCR with a bacterial targeted forward primer (B27f, 59-AGAGTTTGATCCTGGCTCAG-39) and a universal reverse primer (U1492r, 59-GGTTACCTTGT TACGACTT-39). Environmental rRNA clone libraries were constructed by cloning amplicons into a pCR4 TOPO vector and

transforming into chemically competent *Escherichia coli* according to the manufacturer's protocol (TOPO TA cloning kit; Invitrogen Inc.). Transformants were screened on LB-kanamycin-X-Gal plates using blue-white selection. Plasmids were purified with the Montage miniprep kit (Millipore, Inc.) and sequenced with BigDye chemistry (version 3.1) on an ABI 3730 capillary sequencer. Ninety-six plasmids were sequenced and compared in both directions from each anode sample. SSU rRNA sequences were trimmed to remove the vector using Sequencher 4.0 (Gene Codes Inc., Ann Arbor, MI). SSU rRNA sequence data were compiled and aligned to full-length sequences obtained from GenBank with the FASTALIGNER alignment utility of the ARB program package (www.arb-home.de). Alignments were verified by comparison of the sequences of secondary structure with those of *Escherichia coli* and closely related phylotypes. Phylogenetic analysis of the bacterial SSU rRNA sequences was accomplished with MrBayes version 3.1.2.

Results and discussion

Power production

Table 2 and Fig. 5 summarize power and power density for all the BMFC deployments. Power density was normalized to cross-sectional area of the respective designs (0.0062 and 0.4 m²) because this dimension has implications for scaling up the power output of BMFCs through enlargement or by deploying an array of devices. BMFC 1 produced an average power of 0.2 mW (32 mW m⁻²). As in our previous experiments, this design of BMFC did not produce a sustained level of power. It peaked on day 23 at about 0.7 mW (113 mW m⁻²) and then decayed to approximately 0.1 mW (16 mW m⁻²) after day 100. BMFCs 2 and 3 produced significantly more power. The average power for this configuration ($n = 2$) was about 11 ± 1 mW (27 ± 2 mW m⁻²). BMFC 4 produced an average of 56 mW (140 mW m⁻²) over a deployment of 127 days that began at the end of the BMFC 2 deployment.

The power records from the three chamber deployments are highly variable and show normal distributions around the respective mean values with relative standard deviations ranging from 30 to 90%. We speculated in an earlier report⁷ that part of the variability might be due to tidal pumping resulting from transient pressure anomalies and elastic properties of the sediment matrix.^{25,32–34} However, a power spectral density (PSD)³⁵ plot did not show peaks corresponding with a tidal frequency and suggested that the variability was due to random noise. We also attempted a cross-spectral analysis between power and wave height, including a distributed lag analysis to look for delayed effects of pressure gradients, but did not identify any significant

Table 2 Summary of Monterey Canyon fuel cell experiments

	Description	Length of deployment/days	Peak power output/mW	Average power output/mW	Average power density/mW m ⁻²	Rel. St. Dev.
BMFC 1	Anode buried in sediment	162	0.7	0.2	32	76%
BMFC 2	Anode enclosed in chamber	68	20	12	30	38%
BMFC 3	Anode enclosed in chamber	69	20	11	27	90%
BMFC 4	Anode enclosed in chamber	127	80	56	140	30%

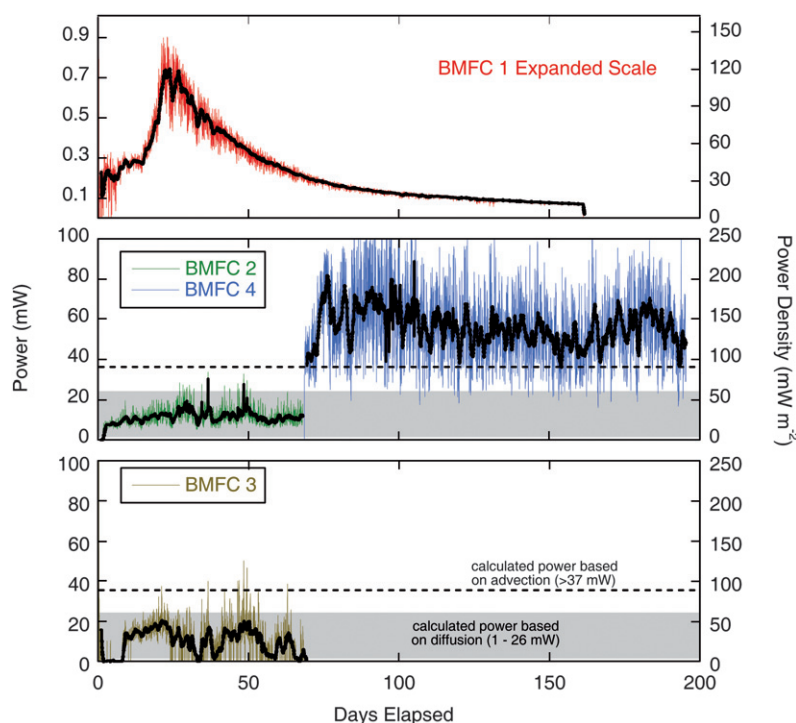


Fig. 5 Power records from all BMFC deployments (raw data is shown with an overlay showing the 24 h running average in bold). Left axis shows actual power output and right axis shows power normalized to cross-sectional area. The upper panel has a magnified scale and shows the BMFC 1 results. Data from BMFCs 2–4 are shown in the lower panels. Shaded area is range of power predicted by diffusion calculations. Dashed line shows lower bound of power expected from advective flux (details in text).

correlation. Wave height data were obtained from NOAA, National Data Buoy Center Site 46042.

The lack of correlation with tides is in contrast to previous findings in Yaquina Bay in which power was correlated and in phase with the tidal signal.⁷ However, Yaquina Bay is an estuary and tidal fluctuations are accompanied by changes in pressure, salinity (and therefore conductivity), dissolved oxygen and temperature. In the deep ocean, tidal fluctuations would only cause pressure changes, which we hypothesized might result in power fluctuations due to changes in seepage rates. Since variations in power were not significantly correlated to tidal pressure, changes in power output are probably due to a combination of factors. Other possible factors that might contribute to the variable power output include environmental factors affecting the cathode, bioirrigation (especially by clams living within the seep sediments), heterogeneous fluid composition, and random stirring events that facilitate transport of electroactive species to the electrode surface.

Electrode potentials

Overpotential is the difference between observed electrode potential and potential at equilibrium conditions.³⁶ Open circuit potentials are always lower than theoretical cell potentials due to overpotentials at the cathode and anode. There are additional current dependent overpotentials at each electrode due to activation losses, bacterial metabolic losses and mass transport (or concentration losses).³⁷ Current dependent overpotentials are the difference between electrode potential at open circuit and under

load. They are useful indicators of which electrode is most affected by current limiting processes (*e.g.*, mass transfer of reactants or passivation) in a given experiment. A departure from zero (positive for the anode and negative for the cathode) is correlated with apparent limitation at the electrode. The BMFCs in this study were not equipped with devices that allowed direct measurements of the open circuit potential of the electrodes (circuits were closed at the time of deployment and remained so for the entire experiment). However, using average open circuit values observed during previous experiments with buried anodes at a nearby seep (-0.43 and 0.38 V vs. Ag/AgCl for the anode and cathode, respectively),²⁰ we can estimate the current dependent overpotentials (potential under load – potential at open circuit, η) for the electrodes in each BMFC (Fig. 6). In doing this we note that from our experience the assumed open circuit values are very typical for sulfide-rich marine sediment/seawater based MFCs ± 0.03 V.⁹ Because the cell potential is maintained at 0.4 V by the potentiostat the difference in overpotentials remains constant.

BMFC 1 began cathode limited and shifted into apparent anode limitation over the course of its deployment. This change can be attributed to a typical 1–2 week period of cathode conditioning during which cathode potential vs. Ag/AgCl rises sigmoidally.²⁰ In contrast, BMFC 2 (and its redeployment as BMFC 4) exhibited slightly greater anode overpotential than cathode overpotential (0.3 V vs. -0.2 V, respectively) during most of the record (the datalogger recording anode potential failed early in the BMFC 4 deployment). BMFC 3 exhibited a systematic progression from predominantly anode limitation

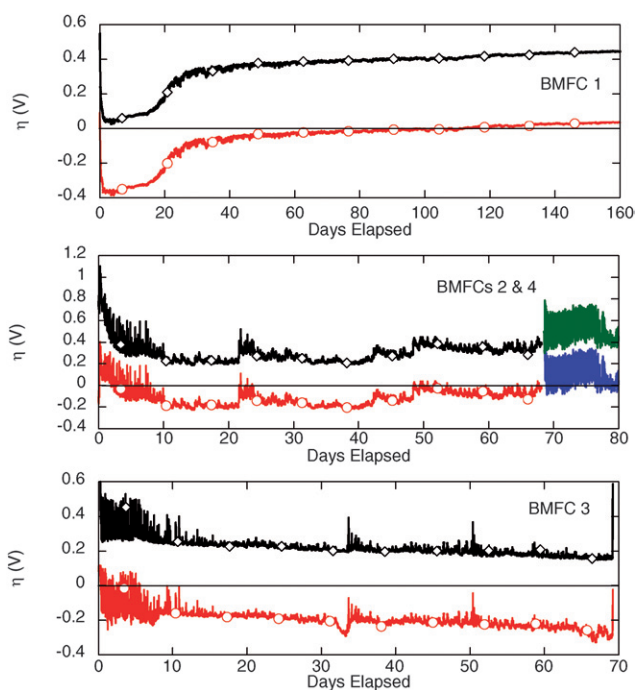


Fig. 6 Cathode (○) and anode (◇) overpotentials (η) for all BMFC deployments based on open circuit potentials (vs. Ag/AgCl) observed during previous experiments at nearby seeps. BMFCs 2 and 4 are shown on the same plot (middle panel) since they are the same device that was recovered and then redeployed. The datalogger monitoring anode potential failed during the BMFC 4 deployment, so the record is incomplete.

towards cathode limitation. The first 10 to 14 days of each chamber deployment shows a noisy signal for both the cathode and anode potential. This characteristic is shared by the data from all of the chamber configurations but is probably not related to electrode conditioning since the chambers were tested in Yaquina Bay prior to the Monterey Canyon deployments. The cause of the noisy signal does not appear to have limited or inhibited the onset of power generation.

Comparison between buried solid anode and chamber design

The average power density from the chambered BMFCs was similar to the power density from the buried anode. However, the chambers had a cross section (or footprint) that was approximately 65 times larger than the buried anode. Thus, in terms of actual power output, the chambered BMFCs produced 60 to 280 times more power than the buried anode BMFC and thus had superior performance according to the criteria of producing useful power for oceanographic sensors. The different designs required similar resources for deployment in terms of ROV time and capacity. Scaling up the solid anode in size or deploying a complex array of them to produce greater power would not be as practical as deploying a single chamber.

The power records from the different BMFC designs have distinct patterns related to the transport processes that control the delivery of electron donors in the sediment and to the anode in the respective BMFCs. The power record from BMFC 1 showed a peak on day 23 followed by a decay over time. This

pattern is similar to previous results²⁰ and is consistent with an electrochemical system for which (1) the cathode requires a conditioning period, (2) long-term power production is limited by anode processes and anode area, and (3) the medium surrounding the anode is stagnant (or unstirred) and thus the electron donor supply is dependent on molecular diffusion in the absence of bioirrigation. In this case the apparent diffusive supply is at odds with the observed seepage from the seafloor. Therefore, we conclude that the solid anode buried in the sediment effectively plugged the advective transport of the seep. Conversely, the records from BMFCs 2–4 show no systematic decay in the amount of power produced over time. For power levels to have remained approximately constant (*i.e.* not decay) we conclude that there was a sustained supply of electron donors to the chambers.

When the spring-loaded check valves on BMFC 2 were replaced with swing check valves, power increased by a factor of five (Table 2, Fig. 5). The other alteration we made at the redeployment was to use syntactic foam to suspend the cathode above the BMFC. However, because BMFC 2 had greater anode overpotential than cathode overpotential we infer that the alteration that affected the anode (changing the valve) probably had a larger effect. The higher power associated with the lower pressure valves suggests that seep fluid was able to pass through the chamber and out the check valves on BMFC 4 (0.7 kPa cracking pressure) but was often restricted by the valves on BMFCs 2 and 3 (3.4 kPa cracking pressure).

The power predictions based on eqns (1) and (2), independent measurements of fluid flow and composition, and BMFC dimensions are consistent with the different transport mechanisms in the sediments beneath the various chambers. We predicted a range of 37 to 112 mW could be sustained by advective fluxes. These predictions bracket the power produced by BMFC 4 but are far greater than what was generated by BMFCs 2 and 3. BMFCs 2 and 3 produced power in the middle of our predicted range (1 to 26 mW) based on diffusive transport of sulfide across the sediment–water interface. However, current was highly variable suggesting advective inputs were at times non-zero.

BMFC efficiency

A common measure of fuel cell efficiency is the amount of electrons passed through the circuit divided by the amount of available electrons added to the system as fuel; this quantity is known as coulombic or current efficiency.^{37,38} Coulombic efficiency is challenging to measure in BMFC field experiments because it is difficult to constrain the delivery of electron donors from the natural system. As noted earlier, predictions for the Monterey Canyon seep environment depend on the presumed transport mechanism and bracket the current and therefore power generated by all the chambered BMFCs. Taking the upper bound of the predicted range (112 mW) and the performance of BMFC 4 gives an efficiency of approximately 50%. This may indicate ~50% of the sulfide (and other electron donors) transported into the chamber exits unreacted. If this is verified in future experiments, the BMFCs can be re-designed to lower the fraction of unreacted electron donor and to produce more power.

Two changes that may lower the fraction of unreacted electron donor are increasing the residence time of fluid in the chamber

(by changing the volume), and/or changing ratio of anode surface area (in m^2) to chamber volume (in L). By comparison, our earlier experiments with mechanically pumped chambered BMFCs in Yaquina Bay had a residence time of approximately 5 h and 26 m^2 of anode area within a 2 L chamber volume (13 : 1 ratio).⁷ In Monterey Canyon (an environment with higher sulfide fluxes) we estimate a residence time of 8–22 h based on fluid flux measurements from Labonte *et al.*,²⁵ and we had 78 m^2 of anode surface area within a 20 L volume (3.9 : 1 ratio). Peak power densities in Yaquina Bay were 380 mW m^{-2} of seafloor during polarization experiments under pumped conditions. The maximum power density observed in the Monterey Canyon experiments was approximately 200 mW m^{-2} . Because this is an environment with a higher flux of sulfide across the sediment–water interface we conclude that the residence time was not as limiting as the ratio of anode surface area to volume. We predict higher power densities may be achieved by increasing the amount of anode area within the chambers to ensure that all the potential electron donors are oxidized before leaving the chamber (assuming advective transport). Improvement may also be achieved by altering anode positioning to insure electrode area is evenly distributed relative to the preferential flow-path through the chamber. This might be accomplished by adding bulkheads within the chamber to direct fluid flow past all of the electrode material.

Performance may also be improved by linking a series of BMFCs rather than scaling up the size of a single device. Aelterman *et al.*³⁹ and Ieropoulos *et al.*⁴⁰ demonstrated the benefits of connecting laboratory fuel cells in series or parallel to boost voltage or current, respectively. In the latter case, the authors conclude that compartmentalizing a fuel cell into many units results in more efficient operation than a single large unit. In oceanic settings the entire fuel cell is immersed in conductive fluid and electrode pairs cannot be isolated from one another so they cannot be connected in series. Multiple distinct fuel cells could be linked together in parallel to boost current¹⁸ but it is unknown how BMFCs in such a configuration would affect each other (if at all). The higher power density from our Yaquina Bay experiments compared to our Monterey Canyon experiments is consistent with the observation that smaller BMFCs may be inherently more efficient than larger BMFCs. However, based on the metric of producing enough power to operate an instrument, the larger fuel cell was the best performer.

Each chamber deployment exhibited some degree of cathode limitation as evidenced by current dependent overpotentials reaching -0.3 V (Fig. 6). This result is not surprising since bottom seawater in Monterey Canyon is very low in dissolved oxygen ($11 \mu\text{M}$) and bottom currents are relatively slow. One possible solution is to increase the amount of cathode surface area. Other measures that could be considered include catalysts to promote oxygen reduction or reduction of alternative electron acceptors such as nitrate or Mn(IV) .⁴¹ Any alternative catalysts would need to be studied and compared to naturally occurring processes. We also noticed a difference between seeps in this study. BMFC 2 and 4 showed less cathode overpotential than BMFC 3, which showed a constant decline over time. Upon recovery of the BMFCs we noted that the cathode and the outside of BMFC 3 was noticeably more covered with a white bacterial mat that might have been sulfide-oxidizing bacteria. It

is possible that the seep we selected for the BMFC 3 deployment had more diffuse flow than the seep at which BMFC 2 (and then 4) was deployed, resulting in the development of a bacterial mat that progressively fouled the cathode. Therefore, site selection may also play a role in maintaining cathode electroactivity, but this consideration is secondary to the requirement of targeting active seeps in order to maximize delivery of fuel to the anode chamber.

Comparison of microbial communities

Based on the 16s rRNA analysis of clone libraries, which provide a robust index of microbial community composition, the bacteria within the biofilm on the BMFC 2 anode were dominated by epsilonproteobacteria (Table 3). The phylotypes recovered from the BMFC 4 anode were significantly more varied in phylogenetic diversity and contained sequences allied to the deltaproteobacteria, epsilonproteobacteria, and flavobacterium/cytophaga/bacteriodes (FCB).

The difference in phylogenetic diversity between BMFC 2 and 4 likely reflects different chemical environments inside the respective anode chambers. For BMFC 2, we have shown that the fuel delivery to the chamber was at a rate in keeping with transport predominantly by diffusion. Without advective flow, the chamber would approximate a batch reactor in which the products of anode reactions accumulate. The dominance of epsilonproteobacteria in BMFC 2 suggests that these organisms

Table 3 Microbial community analysis

Bacterial group	Most closely related species	Proportion of phylotypes found	
		BMFC 2	BMFC 4
Alphaproteobacteria	Roseobacter denitrificans	1%	0%
Betaproteobacteria	Brachymonas denitrificans	1%	6%
Deltaproteobacteria	Desulfobulbus propionicus, Desulfuromonas acetoxidans	1%	23%
Gammaproteobacteria	Solemya reidi symbiont	0%	9%
Epsilonproteobacteria	Arcobacter nitrofigilis	93%	23%
Firmicutes	—	1%	11%
Deferribacteres/ Flexistipes	Flexistipes sinus	2%	0%
Myxobacteria	—	0%	2%
Fusobacter	Propionigenium modestum	0%	4%
Flavobacterium/ cytophaga/bacterioides	Cytophaga fermentans	0%	17%
Mycoplasma	Asteroleplasma	0%	2%
Planctomycetes	Verrucomicrobium	0%	2%

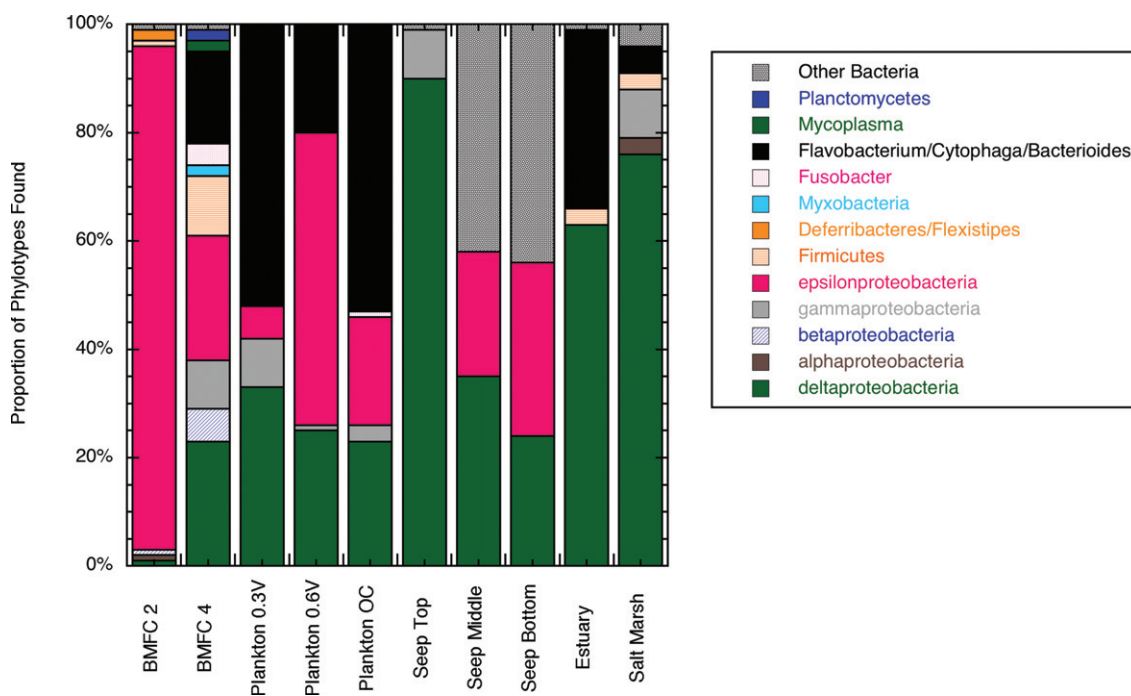


Fig. 7 Comparison of phylogenetic communities found on anodes between this and previous experiments. Plankton data are from experiments at various controlled potentials (OC = open circuit),⁴⁵ seep data are from experiments at a Monterey Canyon cold seep with a vertical buried anode that was sampled at three intervals (20–29 cm, 46–55 cm and 70–76 cm below the sediment–water interface),²⁰ estuary and salt marsh data are from plate anodes buried horizontally in the sediment.⁴⁶

may help drive the electron transfer process in this environment under fuel-limited conditions. In contrast, previous sediment fuel cell experiments have shown that deltaproteobacteria become the dominant phylotype in anode biofilms (Fig. 7). The epsilonproteobacteria were most closely related to *Arcobacter nitrofigilis* which are commonly found at oxygen–sulfide transitions in marine systems.⁴² This association is consistent with our understanding that sulfide is the major electron donor for BMFCs in these environments.

In BMFC 4, it appeared that fluid flowed through the chamber and was episodically refreshed. This configuration led to a more diverse community, possibly due to more concentrated electron donors. The samples recovered from the BMFC 4 anode also included representatives from the FCB groups which are known to process complex organic compounds and produce secondary metabolites that might be used as electron donors for power generation.^{43,44} We cannot be certain about the phylogenetic differences between BMFC 2 and 4 since there are only two samples to compare. However, they suggest a more systematic experiment relating fluid transport, microbial community analysis and power production could produce new insights about the role of certain groups of organisms in benthic fuel cells.

Fig. 7 compares the phylogenetic communities from BMFCs 2 and 4 with other experiments. In all cases shown in the comparison, the phylogenetic communities represent those present at the end of each experiment. In the case of BMFCs 2 and 4 the current being produced at the end of the experiment was representative of the long-term average of what could be produced by these BMFCs. In the other experiments the current profiles were more like BMFC 1 (a peak followed by a decay) and

the communities represent the late-time low-current production phase rather than the peak current phase of the respective experiments. Therefore, the results from the BMFCs described in this paper might implicate new organisms that might participate in current generation that were not previously observed in marine microbial fuel cells (*e.g.* betaproteobacteria and firmicutes groups found on the BMFC 4 anode).

Conclusion

BMFCs with carbon-fiber brush anodes enclosed in chambers and suspended above the sediment water interface clearly outperformed a BMFC with a solid anode buried in the sediment. Based on the configurations in this investigation, 600 solid anodes would be required to generate power equivalent to one chambered BMFC with natural advection. Tender *et al.*¹⁸ described other configurations of solid anodes resulting in more anode surface area per device cross sectional area. However, it is unknown how their design might benefit, if at all, from advective processes in the sediment. Even under low-flow conditions (BMFCs 2 and 3) the chamber design behaved more like a well-mixed reactor in which the geochemical gradient of electron donors was maintained. The solid anode BMFC exhibited the characteristics of an unstirred reactor in which the concentration gradient of the electron donor away from the anode diminishes due to progressive depletion of electron donors around the anode.

One of the deployments produced an average of 56 mW of power, which is enough to power some off the shelf low-power oceanographic instruments. Lowering the power demands of

sensors by adjusting their duty cycles is a way to increase the number and types of sensors that can practicably be powered by BMFCs. A remaining obstacle is that BMFCs generate power at a low voltage (0.4 V in these experiments) and instruments typically require higher voltage inputs (3.5 V and greater) thus requiring a DC–DC converter to step up the voltage.¹⁸ We have already begun new experiments that include investigation of these devices coupled to BMFCs.

Acknowledgements

This research was supported by award No. N00014-06-1-0212 from the U.S. Office of Naval Research. We are grateful to Monterey Bay Aquarium Research Institute, the crew of the Pt. Lobos and the pilots of the ROV Ventana for skillful and safe deployments. This paper was improved by helpful comments from J. Westall and an anonymous reviewer.

References

- C. E. Reimers, L. M. Tender, S. Fertig and W. Wang, *Environ. Sci. Technol.*, 2001, **35**, 192–195.
- L. M. Tender, C. E. Reimers, H. A. Stecher, D. E. Holmes, D. R. Bond, D. A. Lowy, K. Pilobello, S. J. Fertig and D. R. Lovley, *Nat. Biotechnol.*, 2002, **20**, 821–825.
- D. R. Bond, D. E. Holmes, L. M. Tender and D. R. Lovley, *Science*, 2002, **295**, 483–485.
- D. R. Lovley, *Curr. Opin. Biotechnol.*, 2006, **17**, 327–332.
- D. A. Lowy, L. M. Tender, J. G. Zeikus, D. H. Park and D. R. Lovley, *Biosens. Bioelectron.*, 2006, **21**, 2058–2063.
- R. Farzaneh, T. L. Richard, R. A. Brennan and B. E. Logan, *Environ. Sci. Technol.*, 2007, **41**, 4053–4058.
- M. E. Nielsen, C. E. Reimers and H. A. Stecher, *Environ. Sci. Technol.*, 2007, **41**, 7895–7900.
- C. Dumas, A. Mollica, D. Feron, R. Basseguy, L. Etcheverry and A. Bergel, *Electrochim. Acta*, 2007, **53**, 468–473.
- N. Ryckelynck, H. A. Stecher and C. E. Reimers, *Biogeochemistry*, 2005, **76**, 113–139.
- S. K. Chaudhuri and D. R. Lovley, *Nat. Biotechnol.*, 2003, **21**, 1229–1232.
- D. R. Lovley, *Nat. Rev. Microbiol.*, 2006, **4**, 497–508.
- D. R. Bond and D. R. Lovley, *Appl. Environ. Microbiol.*, 2003, **69**, 1548–1555.
- D. E. Holmes, S. K. Chaudhuri, K. P. Nevin, T. Mehta, B. A. Methe, A. Liu, J. E. Ward, T. L. Woodard, J. Webster and D. R. Lovley, *Environ. Microbiol.*, 2006, **8**, 1805–1815.
- D. E. Holmes, J. S. Nicoll, D. R. Bond and D. R. Lovley, *Appl. Environ. Microbiol.*, 2004, **70**, 6023–6030.
- G. Reguera, K. P. Nevin, J. S. Nicoll, S. F. Covalla, T. L. Woodard and D. R. Lovley, *Appl. Environ. Microbiol.*, 2006, **72**, 7345–7348.
- U. Schröder, *Phys. Chem. Chem. Phys.*, 2007, **9**, 2619–2629.
- A. Shantaram, H. Beyenal, R. Raajan, A. Veluchamy and Z. Lewandowski, *Environ. Sci. Technol.*, 2005, **39**, 5037–5042.
- L. M. Tender, S. A. Gray, E. Groveman, D. A. Lowy, P. Kauffman, J. Melhado, R. C. Tyce, D. Flynn, R. Petrecca and J. Dobarro, *J. Power Sources*, 2008, **179**, 571–575.
- B. E. Logan and J. M. Regan, *Environ. Sci. Technol.*, 2006, **40**, 5172–5180.
- C. E. Reimers, P. Girguis, H. A. Stecher, L. M. Tender and N. Ryckelynck, *Geobiology*, 2006, **4**, 123–136.
- J. P. Barry, H. G. Greene, D. L. Orange, C. H. Baxter, B. H. Robison, R. E. Kochevar, J. W. Nybakken, D. L. Reed and C. M. McHugh, *Deep-Sea Res., Part I: Oceanographic Research Papers*, 1996, **43**, 1739–1762.
- D. L. Orange, H. G. Greene, D. Reed, J. B. Martin, C. M. McHugh, W. B. F. Ryan, N. Maher, D. Stakes and J. Barry, *Geol. Soc. Am. Bull.*, 1999, **111**, 992–1009.
- C. K. Paull, B. Schlining, W. Ussler, J. B. Paduan, D. Caress and H. G. Greene, *Geology*, 2005, **33**, 85–88.
- J. B. Martin, D. L. Orange, T. D. Lorenson and K. A. Kvenvolden, *J. Geophys. Res.: Solid Earth*, 1997, **102**, 24903–24915.
- A. L. LaBonte, K. M. Brown and M. D. Tryon, *J. Geophys. Res.: Solid Earth*, 2007, 112.
- B. P. Boudreau, *Diagenetic models and their implementation: modelling transport and reactions in aquatic sediments*, Springer-Verlag, Heidelberg, 1997.
- H. D. Schulz, in *Marine Geochemistry*, ed. H. D. Schulz and M. Zabel, Springer, Berlin, Editon edn, 2006.
- C. E. Reimers, R. A. Jahnke and D. McCorkle, *Global Biogeochem. Cycles*, 1992, **6**, 199–224.
- A. E. Rathburn, M. E. Perez, J. B. Martin, S. A. Day, C. Mahn, J. Gieskes, W. Ziebis, D. Williams and A. Bahls, *Geochem. Geophys. Geosyst.*, 2003, 4.
- O. Hasvold, H. Henriksen, E. Melvaer, G. Citi, B. O. Johansen, T. Kjonigsen and R. Galetti, *J. Power Sources*, 1997, **65**, 253–261.
- P. R. Girguis, V. J. Orphan, S. J. Hallam and E. F. DeLong, *Appl. Environ. Microbiol.*, 2003, **69**, 5472–5482.
- T. E. Jupp and A. Schultz, *J. Geophys. Res.: Solid Earth*, 2004, 109.
- M. K. Tivey, A. M. Bradley, T. M. Joyce and D. Kadko, *Earth Planet. Sci. Lett.*, 2002, **202**, 693–707.
- K. L. Wang and E. E. Davis, *J. Geophys. Res.: Solid Earth*, 1996, **101**, 11483–11495.
- M. Trauth, *MATLAB Recipes for Earth Sciences*, Springer, 2006.
- A. J. Bard and L. R. Faulkner, *Electrochemical Methods*, John Wiley & Sons, Inc., New York, 2nd edn, 2001.
- B. E. Logan, B. Hamelers, R. Rozendal, U. Schröder, J. Keller, S. Freguia, P. Aelterman, W. Verstraete and K. Rabaey, *Environ. Sci. Technol.*, 2006, **40**, 5181–5192.
- N. Kim, Y. Choi, S. Jung and S. Kim, *Biotechnol. Bioeng.*, 2000, **70**, 109–114.
- P. Aelterman, K. Rabaey, H. T. Pham, N. Boon and W. Verstraete, *Environ. Sci. Technol.*, 2006, **40**, 3388–3394.
- I. Ieropoulos, J. Greenman and C. Melhuish, *Int. J. Energy Res.*, 2008, DOI: 10.1002/er.1419.
- A. Rhoads, H. Beyenal and Z. Lewandowski, *Environ. Sci. Technol.*, 2005, **39**, 4666–4671.
- B. J. Campbell, A. S. Engel, M. L. Porter and K. Takai, *Nat. Rev. Microbiol.*, 2006, **4**, 458–468.
- J. S. Covert and M. A. Moran, *Aquat. Microbial Ecol.*, 2001, **25**, 127–139.
- D. L. Kirchman, *FEMS Microbiol. Ecol.*, 2002, **39**, 91–100.
- C. E. Reimers, H. A. Stecher, J. C. Westall, Y. Alleau, K. A. Howell, L. Soule, H. K. White and P. R. Girguis, *Appl. Environ. Microbiol.*, 2007, **73**, 7029–7040.
- D. E. Holmes, D. R. Bond, R. A. O'Neill, C. E. Reimers, L. R. Tender and D. R. Lovley, *Microb. Ecol.*, 2004, **48**, 178–190.